

The Effect of User Distribution on a Linear Cellular Multiple-Access Channel

Symeon Chatzinotas, Muhammad Ali Imran, Costas Tzaras

Centre for Communication Systems Research

University of Surrey, United Kingdom, GU2 7XH

Email: {S.Chatzinotas, M.Imran, C.Tzaras}@surrey.ac.uk

Abstract—The Gaussian Cellular Multiple-Access Channel (GCMAC) has been the starting point for studying the Shannon-theoretic limits of cellular systems. In 1994, a simple infinite GCMAC was initially introduced by Wyner and was subsequently extended by researchers to incorporate flat fading environments and power-law path loss models. However, Wyner-like models, preserve a fundamental assumption, namely the symmetry of User Terminals (UTs). In this paper, we investigate the effect of this assumption on the sum-rate capacity limits, by examining the case of distributed and thus asymmetric UTs. The model under investigation is a GCMAC over a linear cellular array in the presence of power-law path loss and flat fading. In this context, we study the effect of UT distribution for cell-centre and cell-edge UTs and we show that its effect is considerable only in the case of low cell density.

Multicell Decoding; Cellular Gaussian Multiple-Access Channel; User Distribution

I. INTRODUCTION

The Gaussian Cellular Multiple-Access Channel (GCMAC) has been the starting point for studying the Shannon-theoretic limits of cellular systems. In 1994, a simple infinite GCMAC was initially introduced by Wyner [1] in order to derive closed-form formulas for sum-rate uplink capacity. Subsequently during the last decade, Wyner's model has been extended to incorporate flat fading environments in [2] and power-law path loss models in [3]. However, in both of these extensions a fundamental assumption of Wyner's model has been preserved, namely the symmetry of User Terminals (UTs). UT symmetry implies that the UTs of each cell are collocated or positioned equidistantly from the Base Station (BS) and thus they are equally affected by path loss. In this paper, we investigate the effect of distributed and thus asymmetric UTs on the fundamental capacity limits of cellular systems. The model under investigation is a GCMAC over a linear cellular array in the presence of power-law path loss and Rayleigh flat fading. The outline of this paper is as follows: Section II presents a brief comparison of the already existing "collocated" models.

The work reported in this paper has formed part of the "Fundamental Limits to Wireless Network Capacity" Elective Research Programme of the Virtual Centre of Excellence in Mobile & Personal Communications, Mobile VCE, www.mobilevce.com. This research has been funded by the following Industrial Companies who are Members of Mobile VCE - BBC, BT, Huawei, Nokia, Nokia Siemens Networks, Nortel, Vodafone. Fully detailed technical reports on this research are available to staff from these Industrial Members of Mobile VCE.

Subsequently, section III describes thoroughly the employed model, as well as the main theorems used for the derivations. Section IV presents the main results in the form of plots and analytical formulas and applies the findings to a practical macrocellular scenario. Finally, section V contains a conclusive summary of this work.

II. RELATED WORK

In the following formulations, D is the coverage range of the linear cellular system, N is the number of BSs, K is the number of UTs per cell and η is the power-law path loss exponent. Under these assumptions, $\Pi = N/D$ represents the cell density of the cellular system and R represents the cell radius. Throughout this paper, $\mathbb{E}[\cdot]$ denotes the expectation, $(\cdot)^*$ denotes the complex conjugate, $(\cdot)^\dagger$ denotes the Hermitian matrix and \odot denotes the Hadamard product. $\Pi(t/T)$ is the rect function, where T is the width of the pulse. The figure of merit studied in this paper is the per-cell sum-rate capacity achieved with multicell decoding, which is denoted by C_{opt} . It should be noted that in the context of hyper-receiver cellular networks, all the UT signals received by the BSs of the system are transmitted to a central location (hyper-receiver) for joint processing (multicell decoding) [1] and therefore intercell interference does not have a negative effect on the capacity of the cellular system.

Wyner's model [1] assumes that all the UTs in the cell of interest have equal channel gains which are normalized to 1. It considers interference only from the users of the two neighboring cells, which are assumed to have a fixed channel gain, also known as interference factor α . Assuming that there is a power-law path loss model which affects the channel gain, then Wyner has modeled the case where the UTs of each cell are symmetric, since no decrease of the channel gain with distance is considered. The same assumption is made by Somekh-Shamai [2], which have extended Wyner's model for flat fading environment. In both [1] and [2], a single interference factor α is utilized to model both the cell density and the path loss. The interference factor α ranges in $[0, 1]$, where $\alpha = 0$ represents the case of perfect isolation among the cells (i.e. $\Pi \ll 1$ and $\eta \gg 1$) and $\alpha = 1$ represents the case of BSs' collocation, namely a SIMO MAC channel (i.e. $\Pi \gg 1$). The case $\eta \ll 1$ does not correspond to a realistic

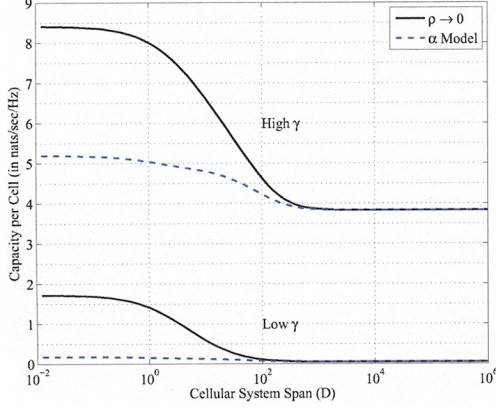


Fig. 1. Capacity per cell C (nat/s/Hz) vs. cellular system range D for Letzepis' model (solid lines) and Wyner-like models (dashed lines). Parameter values $N = 100$, $\eta = 2$, $K = 5$, Low $\gamma = .01$ and High $\gamma = 10$.

scenario, because η typically ranges between 2 and 5 for real-world cellular systems [4].

The model proposed by Letzepis in [3] differs from the aforementioned models in the sense that it considers interference from all the UTs of the cellular system. For the UTs of each cell, an interference coefficient is defined w.r.t. each BS, which depends on the power-law path loss model. Although Letzepis takes into account the path loss effect, the UTs of each cell have still equal channel gains and this models the case where the UTs of each cell are symmetric. However, this model is more detailed than the previously described models, since it decomposes the interference factor α , so that the cell density Π and the path loss exponent η can be modelled and studied separately. According to this model, the received signal at cell n for the flat fading case is:

$$y_i^n = \sum_{k=1}^K b_{ki}^n x_{ki}^n + \sum_{j=1}^{N/2} \alpha_j \left(\sum_{k=1}^K c_{kij}^n x_{kij}^{n-j} + \sum_{k=1}^K d_{kij}^n x_{kij}^{n+j} \right) + z_i^n \quad (1)$$

where x_{ki}^n is the i th complex channel symbol of the k th UT in the n th cell and $\{b_{ki}^n\}$, $\{c_{kij}^n\}$, $\{d_{kij}^n\}$ are independent, strictly stationary and ergodic complex random processes in the time index i , which represent the flat fading processes experienced by the UTs. The fading coefficients are normalized to unit power, i.e. $\mathbb{E}[b_{ki}^n b_{ki}^{n*}] = \mathbb{E}[c_{kij}^n c_{kij}^{n*}] = \mathbb{E}[d_{kij}^n d_{kij}^{n*}] = 1$ and all UTs are subject to an average power constraint, i.e. $\mathbb{E}[x_{ki}^n x_{ki}^{n*}] \leq P$ for all (n, k) . The variable z^n is a c.c.s. random variable representing AWGN with mean $\mathbb{E}[z^n] = 0$ and variance $\mathbb{E}[z^n z^{n*}] = \sigma^2$. The parameter $\gamma = P/\sigma^2$ is defined as the UT transmit power normalized with the receiver noise power. The interference factors α_j of the $n-j$ and $n+j$ cells are calculated according to the "modified" power-law path loss model [5], [3]:

$$\alpha_j = (1 + j/\Pi)^{-\eta/2}. \quad (2)$$

Based on the model of Equation (1), Fig. 1 (solid lines) depicts the high and low- γ per cell capacity for varying cell

densities. The dashed lines of Fig. 1 represents the high and low- γ per-cell capacity, if the model of Equation (1) is modified to comply with the main assumption of Wyner-like models, according to which intercell interference is received only by the first tier of adjacent cells. As expected, for high cell densities (small D) this assumption does not hold and the capacity gap between the two models increases. For low- γ regime, the capacity gap becomes proportionally even larger, as it can be seen in Fig. 1. However, for low cell densities (large D) the two models converge, since the main part of the interference comes from the first tier of neighboring cells. In other words, interference factors α_j for $j > 1$ become insignificant and can be ignored without having an effect on the sum-rate capacity.

III. MODEL DESCRIPTION AND ANALYSIS

The model utilized in this paper to investigate the effect of user distribution is a GMAC over a linear circular cellular array in the presence of power-law path loss and Rayleigh flat fading. The analysis of the planar array can be found in [6]. The current model takes after the model used in [3], as it takes into account interference from all the UTs of the cellular system, scaled according to the employed power-law path loss model. However, it differs significantly from [3] in the sense that the symmetric UTs are replaced by distributed UTs. The channel of a linear cellular array can be modelled as a vector memoryless channel of the form $\mathbf{y} = \mathbf{H}\mathbf{x} + \mathbf{z}$, where the vector $\mathbf{y} = [y^1 \dots y^N]^T$ represents receive signals by the BSs, the vector $\mathbf{x} = [x_1^1 \dots x_K^N]^T$ represents transmit signals by all the UTs of the cellular system and the vector $\mathbf{z} = [z^1 \dots z^N]^T$ represents the i.i.d. Gaussian noise with $\mathbb{E}[\mathbf{z}\mathbf{z}^\dagger] = \sigma^2$. According to [7], if \mathbf{H} denotes the channel matrix of the model, then the asymptotic sum-rate capacity C_{opt} is given by

$$\begin{aligned} C_{\text{opt}} &= \lim_{N \rightarrow \infty} \frac{1}{N} \mathcal{I}(\mathbf{x}; \mathbf{y} | \mathbf{H}) \\ &= \lim_{N \rightarrow \infty} \mathbb{E} \left[\frac{1}{N} \sum_{i=1}^N \log \left(1 + \frac{\tilde{\gamma}}{K} \lambda_i \left(\frac{1}{N} \mathbf{H}\mathbf{H}^\dagger \right) \right) \right] \\ &= \int_0^\infty \log \left(1 + \frac{\tilde{\gamma}}{K} x \right) dF_{\frac{1}{N} \mathbf{H}\mathbf{H}^\dagger}(x) \\ &= \mathcal{V}_{\frac{1}{N} \mathbf{H}\mathbf{H}^\dagger}(\tilde{\gamma}/K) = K \mathcal{V}_{\frac{1}{N} \mathbf{H}^\dagger \mathbf{H}}(\tilde{\gamma}/K) \end{aligned} \quad (3)$$

where $\tilde{\gamma} = KNP/\sigma^2 = KN\gamma$ is the system transmit power normalized by the receiver noise power σ^2 . The term $\lambda_i(\mathbf{X})$ denotes the eigenvalues of matrix \mathbf{X} and $\mathcal{V}_{\mathbf{X}}$ is the Shannon transform with parameter γ of a random square Hermitian matrix \mathbf{X} , where $F_{\mathbf{X}}(x)$ is the cumulative function of the asymptotic eigenvalue distribution (a.e.d.) of matrix \mathbf{X} [7]. For a rectangular Gaussian matrix $\mathbf{G} \sim \mathcal{CN}(\mathbf{0}, \mathbf{I})$ with β being the columns/rows ratio, the a.e.d. of $\frac{1}{N} \mathbf{G}^\dagger \mathbf{G}$ converges almost surely (a.s.) to the nonrandom a.e.d. of the Marčenko-Pastur law

$$\mathcal{V}_{\frac{1}{N} \mathbf{G}^\dagger \mathbf{G}}(\gamma) \xrightarrow{\text{a.s.}} \mathcal{V}_{\text{MP}}(\gamma, \beta) \quad (4)$$

$$\text{where } \mathcal{V}_{\text{MP}}(\gamma, \beta) = \log \left(1 + \gamma - \frac{1}{4} \phi(\gamma, \beta) \right) + \frac{1}{\beta} \log \left(1 + \gamma\beta - \frac{1}{4} \phi(\gamma, \beta) \right) - \frac{1}{4\beta\gamma} \phi(\gamma, \beta) \quad (5)$$

$$\text{and } \phi(\gamma, \beta) = \left(\sqrt{\gamma(1+\sqrt{\beta})^2 + 1} - \sqrt{\gamma(1-\sqrt{\beta})^2 + 1} \right)^2. \quad (6)$$

However, in a power-law path loss environment the channel matrix is given by $\mathbf{H} = \mathbf{\Sigma} \odot \mathbf{G}$, where $\mathbf{\Sigma}$ is a $N \times KN$ deterministic matrix which includes the variance of the fading coefficients for all BS-UT pairs. In Wyner-like models, the $\mathbf{\Sigma}$ matrix is square tridiagonal circulant, whereas in Letzepis' model is just square circulant. The squarity is due to the fact that the symmetric UTs can be grouped and represented as a single UT transmitting with the sum of their power. However, in the current model, the $\mathbf{\Sigma}$ matrix is rectangular block-circulant due to the user spatial distribution. In the context of our asymptotic analysis, the entries of the $\mathbf{\Sigma}$ matrix are defined by the variance profile function $\varsigma(r, t)$ –where $r \in [0, 1]$ and $t \in [0, K]$ are the normalized indexes for the BSs and the UTs respectively. In a power-law path loss environment, this function is given by

$$\varsigma(d(t)) = (1 + d(t))^{-\eta/2} \quad (7)$$

where $d(t)$ is a function mapping the normalized UT index $t \in [0, K]$ to a certain distance $d \in [-D/2, D/2]$ from the BS of interest. According to the Marčenko-Pastur Law approximation in [3], the limiting eigenvalue distribution of $(1/N)\mathbf{H}^\dagger \mathbf{H}$ and its Shannon transform can be approximated by a scaled Marčenko-Pastur law

$$\mathcal{V}_{\frac{1}{N}\mathbf{H}^\dagger \mathbf{H}}\left(\frac{\tilde{\gamma}}{K}\right) \simeq \mathcal{V}_{\text{MP}}(q_K(\mathbf{\Sigma})\frac{\tilde{\gamma}}{K}) \quad (8)$$

where $q(\mathbf{\Sigma}) \triangleq \|\mathbf{\Sigma}\|^2 / KN^2$ with $\|\mathbf{\Sigma}\| \triangleq \sqrt{\text{tr}\{\mathbf{\Sigma}^\dagger \mathbf{\Sigma}\}}$ being the Frobenius norm of the $\mathbf{\Sigma}$ matrix. In the asymptotic regime, the channel matrix is row-regular [7, Definition 2.10] and therefore:

$$\lim_{N \rightarrow \infty} q(\mathbf{\Sigma}) = \frac{1}{K} \int_0^K \varsigma^2(t) dt, \forall r \in [0, 1]. \quad (9)$$

Since the linear array is circular, $\varsigma(d(t))$ will be symmetric about the axis $t = K/2$ and hence Equation (9) can be further simplified to

$$\lim_{N \rightarrow \infty} q(\mathbf{\Sigma}) = \frac{2}{K} \int_0^{K/2} \varsigma^2(d(t)) dt. \quad (10)$$

User distribution effectively alters $d(t)$ and therefore it modifies the variance profile function $\varsigma(d(t))$ and the resulting sum-rate capacity given by Equation (3).

According to [3], this approximation holds for UTs collocated with the BS. However, in this paper analysis and simulations show that the approximation also holds for distributed UTs, providing a useful tool for incorporating user distribution

in information-theoretic cellular models. Furthermore, in [8] it is stated that the limiting eigenvalue distribution converges to the Marčenko-Pastur law, as long as $\mathbf{\Sigma}$ is asymptotically doubly-regular [7, Definition 2.10]. In this paper, it is shown that on the grounds of free probability, the Marcenko-Pastur law can be effectively utilized in cases where $\mathbf{\Sigma}$ is asymptotically row-regular only. The per-cell sum-rate capacity of the current model can be calculated based on the following theorem.

Theorem 1: Let us assume that the transmitters of each cell are positioned on a grid generated according to an invertible Cumulative Distribution Function (CDF) $F_u(r)$, where $r \in [0, 1]$ corresponds to the normalized single-cell distance from the BS. If $\varsigma(d(t))$ is the variance profile function w.r.t. the distance d , then the variance profile function $\tilde{\varsigma}(t)$ w.r.t. the normalized index t of the distributed users is given by

$$\tilde{\varsigma}(t) = \varsigma \left(\sum_{i=-\frac{N}{2}}^{\frac{N}{2}} \left(\frac{1}{2\Pi} \tilde{F}_u^{-1} \left(N \frac{2}{K} t_i \right) + \frac{1}{\Pi} i \right) \cap \left(\frac{t_i}{K/N} \right) \right) \quad (11)$$

$$\tilde{F}_u^{-1} = \begin{cases} F_u^{-1}(d) & d > 0 \\ -F_u^{-1}(-d) & d < 0 \end{cases} \quad \text{and} \quad t_i = t - i \frac{K}{N}$$

where $t \in [0, K/2]$.

Proof: Let's assume that the UTs of each cell are distributed on a regular grid and the points of this grid are generated according to a single-cell probability distribution with a known and invertible CDF $F_u(r)$, $r \in [0, 1]$. The case $r = 0$ corresponds to cell centre transmitters, whereas the case $r = 1$ corresponds to cell edge transmitters. If $x \in [-K/2, K/2]$ is the single-cell UT index ordered w.r.t. the distance d_{sc} from the BS, then

$$d_{sc}(x) = \frac{1}{2\Pi} \tilde{F}_u^{-1} \left(\frac{2}{K} x \right), \tilde{F}_u^{-1} = \begin{cases} F_u^{-1}(d) & d > 0 \\ -F_u^{-1}(-d) & d < 0. \end{cases}$$

The terms $1/2\Pi$ and $2/K$ are normalization factors, due to the fact that $K/2$ UTs are distributed across the cell radius $1/2\Pi$. By using the normalized index $t = x/N$ instead of x ,

$$d_{sc}(t) = \frac{1}{2\Pi} \tilde{F}_u^{-1} \left(N \frac{2}{K} t \right). \quad (12)$$

If the same single-cell distance pattern is reproduced for all N cells of the cellular system, then $d(t)$ is given by

$$d(t) = \sum_{i=-\frac{N}{2}}^{\frac{N}{2}} \left(\frac{1}{2\Pi} \tilde{F}_u^{-1} \left(N \frac{2}{K} t_i \right) + \frac{1}{\Pi} i \right) \cap \left(\frac{t_i}{K/N} \right) \quad (13)$$

where $t_i = t - i \frac{K}{N}$. The factor $\frac{1}{\Pi} i$ compensates for the fact that neighboring BSs are distanced by $\frac{1}{\Pi}$. Knowing the distance of each UT from the BS of interest, the variance profile values for the distributed case can be found by substituting (13) to the variance profile function $\varsigma(d(t))$. ■

In Sec. IV, Theorem 1 is applied to simple user distributions in order to derive some insights on the effect of user distribution on sum-rate capacity. Using the same approach, the

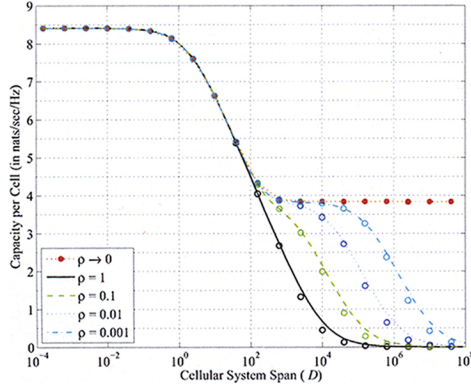


Fig. 2. High- γ capacity per cell C (nat/s/Hz) vs. cellular system coverage D . Parameter values $N = 100, \eta = 2, K = 5, \gamma = 10$.

cellular capacity can be calculated for any one-dimensional user distribution, although the analysis may become tedious and numerical methods may be necessary. It should be noted that the capacity metric C_{opt} calculated using Theorem 1 refers to the expectation of the instant capacity over many random fading realizations and UT positions.

IV. RESULTS

This section presents the analytical capacity results produced by applying Theorem 1 to the uniform user distribution and the truncated uniform distribution for cell-centre and cell-edge users. More specifically, the per-cell sum-rate capacity has been calculated by combining Equations (3), (8), (10) and (11), and it has been plotted w.r.t. a variable cellular system coverage D . All the analytical results are verified by running Monte Carlo simulations over 100 random instances of the system and by averaging the produced results. More specifically, for each system instance the Gaussian complex matrix \mathbf{G} was constructed by randomly generating Gaussian i.i.d. c.c.s. fading coefficients with unit variance. Similarly, the variance profile matrix Σ was constructed by randomly placing the UTs in the segments defined by the user distribution and by calculating the variance profile coefficients using Equation (7). Using the channel matrix $\mathbf{H} = \Sigma \odot \mathbf{G}$, the sum-rate capacity was calculated by evaluating the formula in [9]

$$C_{\text{opt}}(\gamma) = \frac{1}{N} \mathbb{E} [\log \det (\mathbf{I}_N + \gamma \mathbf{H} \mathbf{H}^\dagger)] \quad (14)$$

The simulation points are marked in Fig. 2, 3 by circle points.

Assuming uniformly distributed users, the CDF and its inverse are given by $F_u(r) = F_u^{-1}(r) = r$. Using Theorem 1 and Equation (3), the sum-rate capacity can be plotted as shown in Fig. 2 (solid line). The capacity for high cell densities is identical to the capacity calculated using Letzepis's collocated model. However, for small cell densities the capacity keeps decreasing and for the extreme case of isolated cells, the capacity becomes zero. This phenomenon can be also intuitively explained, since in the asymptotic case, where N is constant and $D \rightarrow \infty$, the distributed users of each cell will be effectively isolated from the BS of the cell.

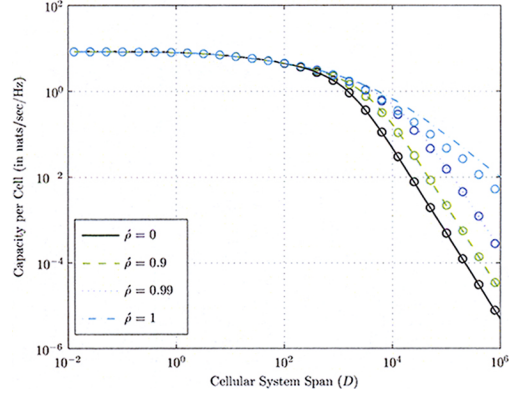


Fig. 3. High- γ capacity per cell C (nat/s/Hz) vs. cellular system coverage D . Parameter values $N = 100, \eta = 2, K = 5, \gamma = 10$.

According to the truncated uniform distribution for cell centre-users, the UTs are uniformly distributed around the BS on a segment of radius $\rho/2\Pi$, where $\rho \in [0, 1]$ is the truncation factor. The setting $\rho = 0$ corresponds to the case where all the users are collocated with the BS and the setting $\rho = 1$ corresponds to the case where UTs are uniformly distributed all over the cell's range. Therefore, the CDF and its inverse for the truncated uniform distribution are given by

$$F_u(r) = \begin{cases} \frac{r}{\rho} & r \in [0, \rho] \\ 0 & r \in [\rho, 1] \end{cases}, F_u^{-1}(r) = \rho r, r \in [0, 1]. \quad (15)$$

Using Theorem 1 and Equation (3), the sum-rate capacity can be plotted as shown in Fig. 2. It can be seen that for high cell densities, the truncation has little effect on the system capacity. This is due to the fact that, in the interfering cells, the variance profile gain from UTs positioned closer to the BS of interest is balanced by the loss from the UTs positioned further from the BS. However, for small densities, the effect of the user distribution is more evident since the received power from the intra-cell UTs becomes dominant.

According to the truncated uniform distribution for cell edge users, the UTs are uniformly distributed around the cell edge on a segment of radius $\hat{\rho}/2\Pi$ where $\hat{\rho} \in [0, 1]$ is the truncation factor. The setting $\hat{\rho} = 0$ corresponds to the case where all the users are collocated at the cell edge and the setting $\hat{\rho} = 1$ corresponds to the case where UTs are uniformly distributed all over the cell's range. Therefore, the CDF and its inverse for the truncated uniform distribution are given by ($r \in [0, 1]$)

$$F_u(r) = \begin{cases} 0 & r \in [0, 1 - \hat{\rho}] \\ \frac{r - 1 + \hat{\rho}}{\hat{\rho}} & r \in [1 - \hat{\rho}, 1] \end{cases}, F_u^{-1}(r) = \hat{\rho} r - \hat{\rho} + 1.$$

Using Theorem 1 and Equation (3), the sum-rate capacity can be plotted as shown in Fig. 3. It can be seen that for high cell densities, the truncation has little effect on the system capacity. For low cell densities, moving the UTs closer to the cell edge results in a higher decrease rate of the capacity. This can be intuitively explained, since in the low cell density regime the

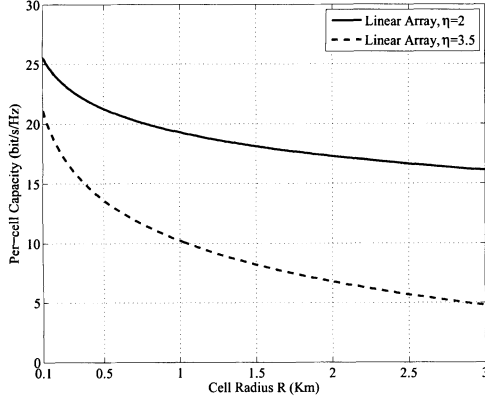


Fig. 4. Per-cell capacity (bit/s/Hz) vs. cell radius R for the linear cellular system. Parameters: $\eta = 2, 3.5$.

intra-cell received power becomes dominant. Therefore, while $\rho \rightarrow 0$ the UTs in the cell of interest become more isolated from the BS, resulting in a lower capacity. However, the effect of the cell-edge truncated uniform distribution is less grave than the effect of the cell-centre truncated uniform distribution. For this reason, the y axes of Fig. 3 have been plotted in logarithmic scale in order to effectively depict the capacity gap in low cell densities.

Subsequently, we discuss the presented results and try to derive some insights on the practical implementation and performance of hyper-receiver cellular networks. In this context, it has been shown that Wyner-like information-theoretic cellular structures can only model the case of low cell density and collocated users. This is due to the fact that in the high cell density regime the assumption of strict first tier interference does not hold. Therefore, Wyner-like models cannot fully exploit the joint-decoding potential of the hyper-receiver and the derived sum-rate capacity is suboptimal. On the other hand, Letzepis's model alleviates the constraining assumption of first tier interference by considering interference from all the users of the cellular system. The derived sum-rate capacity is optimal, but only for the case of collocated users. In the model employed in this paper, the assumption of collocated UTs is alleviated by considering UTs which are identically distributed in each cell. The analysis of this model has shown that UT distribution does not affect the optimal sum-rate capacity in the high cell density regime and thus the same results can be obtained by Letzepis's model. However, this simplification does not apply in the low cell density regime, since the interference factors of adjacent cells become insignificant and the intra-cell received power becomes dominant. From a system-design point of view, this means that the UT distance from the BS of its cell becomes insignificant, since the UT's signal can be adequately received by multiple tiers of adjacent BSs.

In order to derive some practical results about the hyper-receiver capacity performance of real-world macro-cellular systems, the following typical values are used: reference distance $d_0 = 1$ m, UTs per cell $K = 20$, UT transmit power

$P = 200$ mW, thermal noise density $N_0 = -169$ dBm/Hz, channel bandwidth $B = 5$ MHz. In this context, the path loss coefficient is given by $\varsigma = \sqrt{L_0(1 + \frac{d}{d_0})^{-\eta}}$ where d is the distance between the transmitter and the receiver and L_0 is the power degradation due to path loss at the reference distance d_0 . For the purposes of this paragraph, a typical value of $L_0 = -38$ dB for an operating frequency of $f = 1.9$ GHz will be considered [4]. Fig. 4 depicts the per-cell capacity of the linear cellular system versus the cell radius R for a path loss exponent of $\eta = 2$ and 3.5 .

V. CONCLUSION

In this paper, we have investigated the cellular uplink channel in the presence of flat fading, power-law path loss and distributed users. Based on the presented results, it can be seen that user distribution has a different effect on the sum-rate capacity of linear cellular arrays depending on the cell density of the system. This is due to the fact that in distant interfering cells the effect of user distribution is averaged out because of the symmetry of the distribution around the cell centre. However, this is not true for the cell of interest, since user distribution in combination with path loss results in decreased sum-rate capacity. Therefore, in the high cell density regime, where the number of interfering cells is large, user distribution has no effect on sum-rate capacity. On the other hand, in the low cell density regime, where the number of interfering cells is smaller, the intra-cell effect becomes dominant and a decrease on the sum-rate capacity can be observed. The magnitude of the decrease rate is proportional to the distance between the users and the BS, which is determined by the assumed user distribution.

ACKNOWLEDGMENT

The authors would like to thank Prof. G. Caire and Prof. D. Tse for the useful discussions.

REFERENCES

- [1] A. Wyner, "Shannon-theoretic approach to a Gaussian cellular multiple-access channel," *Information Theory, IEEE Transactions on*, vol. 40, no. 6, pp. 1713–1727, Nov 1994.
- [2] O. Somekh and S. Shamai, "Shannon-theoretic approach to a Gaussian cellular multiple-access channel with fading," *Information Theory, IEEE Transactions on*, vol. 46, no. 4, pp. 1401–1425, Jul 2000.
- [3] N. A. Letzepis, "Gaussian cellular multiple access channels," Ph.D. dissertation, Institute for Telecommunications Research, University of South Australia, December 2005.
- [4] T. Rappaport, *Wireless Communications: Principles and Practice*. Upper Saddle River, NJ, USA: Prentice Hall PTR, 2001.
- [5] L. Ong and M. Motani, "On the capacity of the single source multiple relay single destination mesh network," *Ad Hoc Netw.*, vol. 5, no. 6, pp. 786–800, 2007.
- [6] S. Chatzinotas, M. Imran, and C. Tzaras, "Optimal information theoretic capacity of the planar cellular uplink channel," in *9th IEEE International Workshop on Signal Processing Advances in Wireless Communications (SPAWC 2008)*, Recife, Pernambuco, Brazil, Jul 2008.
- [7] A. Tulino and S. Verdú, "Random matrix theory and wireless communications," *Commun. Inf. Theory*, vol. 1, no. 1, pp. 1–182, 2004.
- [8] A. Tulino, S. Verdú, and A. Lozano, "Capacity of antenna arrays with space, polarization and pattern diversity," *Information Theory Workshop, 2003. Proceedings. 2003 IEEE*, pp. 324–327, 31 March–4 April 2003.
- [9] I. E. Telatar, "Capacity of multi-antenna Gaussian channels," *European Transactions on Telecommunications*, vol. 10, no. 6, pp. 585–595, Nov 1999.